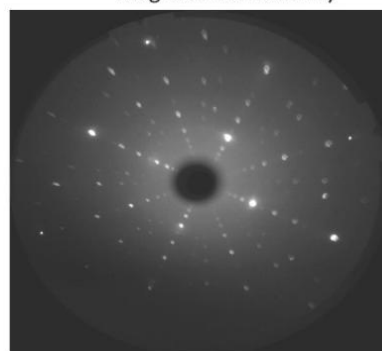
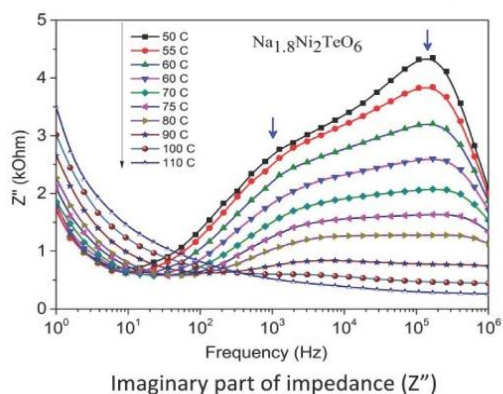
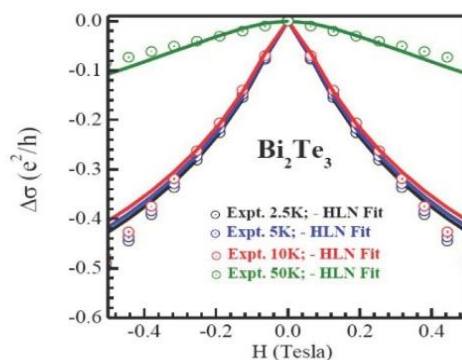
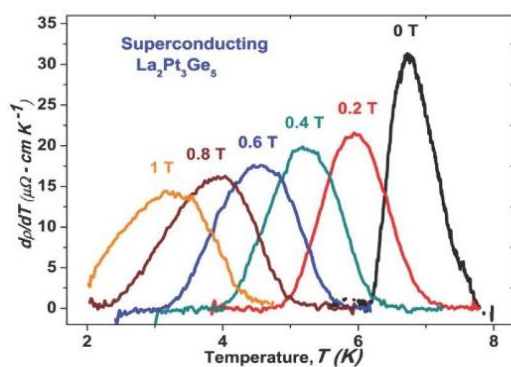


DAE Solid State Physics Symposium 2018

Hisar, Haryana, India • 18–22 December 2018

Editors • Arup Biswas, Veerendra K. Sharma and S. M. Yusuf



Laue diffraction pattern of SnTe(100)

CONTRIBUTED PAPERS

Light up-conversion and structural properties of Sn and Er³⁺ doped Ba_{0.995}Er_{0.005}(Sn_{0.06}Ti_{0.94})O₃ ceramics

Mohd. Azaj Ansari; K. Sreenivas

AIP Conf. Proc. 2115, 030001 (2019) <https://doi.org/10.1063/1.5112840>

Volume 2115 Issue 1 | AIP Conference Proceedings | AIP Publishing

Abstract

View article

PDF

Influence of thermal annealing on phase transformation in Bi₁₀As₄₀Se₅₀ thin films

Mukta Behera; N. C. Mishra; R. Naik

AIP Conf. Proc. 2115, 030002 (2019) <https://doi.org/10.1063/1.5112841>

Abstract

View article

PDF

Pressure induced re-entrant order-disorder like structural phase transition in spinel ferrite nanoparticles

Shekhar Tyagi; Ajay K. Rathore; Gaurav Sharma; Binoy Krishna De; Vivek Dwij; Hemant Singh Kunwar; V. G. Sathe

AIP Conf. Proc. 2115, 030003 (2019) <https://doi.org/10.1063/1.5112842>

Abstract

View article

PDF

Crystal structure of Sb₈Te₃ and Sb₁₀Te₃

C. Rangasami

AIP Conf. Proc. 2115, 030004 (2019) <https://doi.org/10.1063/1.5112843>

Abstract

View article

PDF

Volume 2115 Issue 1 | AIP Conference Proceedings | AIP Publishing

Theoretical prediction of high pressure phase transition and elastic properties of Samarium arsenide (SmAs)

Namrata Yaduvanshi; Shilpa Kapoor; Sadhna Singh

AIP Conf. Proc. 2115, 030005 (2019) <https://doi.org/10.1063/1.5112844>

Abstract

View article

PDF

Coexistence of relaxor and normal ferroelectrics in (Ba_{0.82}Sr_{0.02}Ca_{0.16})Ti_{0.9}Zr_{0.1}O₃

Tusita Sau; Poonam Yadav; N. P. Lalla

AIP Conf. Proc. 2115, 030006 (2019) <https://doi.org/10.1063/1.5112845>

Abstract

View article

PDF

Pressure induced phase transition in U₂C₃ under pressure: An *ab-initio* investigation

B. D. Sahoo; K. D. Joshi; T. C. Kaushik

AIP Conf. Proc. 2115, 030007 (2019) <https://doi.org/10.1063/1.5112846>

Abstract

View article

PDF

Electrical properties of $\text{Ba}(\text{Ni}_{1/3}\text{Ti}_{1/3}\text{W}_{1/3})\text{O}_3$ ceramic 𐄂

Prabhasini Gupta; P. K. Mahapatra; R. N. P. Choudhary

AIP Conf. Proc. 2115, 030015 (2019) <https://doi.org/10.1063/1.5112854>

Abstract 𐄂

View article

PDF

Spin-1 bosons in optical superlattice 𐄂

Chetana G. F. Gaonker; B. K. Alavani; A. Das; R. V. Pai

AIP Conf. Proc. 2115, 030016 (2019) <https://doi.org/10.1063/1.5112855>

Volume 2115 Issue 1 | AIP Conference Proceedings | AIP Publishing

Abstract 𐄂

View article

PDF

Preparation of low-cost porous mullite balls from kaolin and alumina using naphthalene as pore-former 𐄂

Amit Kumar Yadav; Lubna Farheen; Sunipa Bhattacharyya

AIP Conf. Proc. 2115, 030017 (2019) <https://doi.org/10.1063/1.5112856>

Abstract 𐄂

View article

PDF

Theoretical and experimental investigation of different phases in as cast equiatomic CrFeMoNbV alloys 𐄂

A. Saikumaran; R. Mythili; S. Saroja; K. A. Irshad; S. Kalavathy; Rajesh Ganesan

AIP Conf. Proc. 2115, 030018 (2019) <https://doi.org/10.1063/1.5112857>

Abstract 𐄂

View article

PDF

Spin-1 Bosons in optical superlattice

Chetana G.F. Gaonker^{1,a)}, B. K. Alavani¹, A. Das² and R. V. Pai¹

¹Department of Physics, Goa University, Taleigao Plateau, Goa 403206

²Department of Physics, Parvatibai Chowgule College of Arts and Science, Gogol, Margao, Goa 403602

^{a)} physics.chetana@unigoa.ac.in

Abstract. In this paper, we analyze superfluid, insulator and various magnetic phases of ultracold spin-1 bosonic atoms in two-dimensional optical superlattices. Our studies have been performed using Cluster Mean Field Theory. Calculations have been carried out for a wide range of densities and the energy shifts due to the superlattice potential. We find superlattice potential do not change the symmetry of the polar superfluid phases. Superlattice potentials induce Mott insulator phases with half-integer densities. The phase diagram is obtained using superfluid density, nematic order and singlet density. Second order Rényi entanglement entropy is also calculated in different phases. The results show that Rényi entanglement entropy is large in the nematic Mott insulator phase.

INTRODUCTION

Ultracold atoms in optical lattices and superlattices provide us with the realization of engineered quantum many-body lattice models [1]. One remarkable development in this context is the realization of Bose gases in the optical lattices. Superfluid (SF) to Mott Insulator (MI) quantum phase transition in cold bosonic atoms has received great scientific attention since its theoretical prediction in the context of Bose Hubbard model (BHM), and followed by its experimental realization [2-4]. When traps are purely optical, Alkali atoms like ⁸⁷Rb, ²³Na and ⁴⁰K, with hyperfine spin F=1, have spin degrees of freedom and thus, the interaction between bosons is spin-dependent [5]. The interaction is ferromagnetic (e.g. ⁸⁷Rb) or anti-ferromagnetic (e.g. ²³Na), depending upon scattering lengths of singlet and quintuplet channels [6]. The spin-dependent interaction in spinor gases exhibits richer quantum effects than their single-component counterparts and it not only modifies the nature of phase diagrams but also allows the study of superfluidity and magnetism.

The optical superlattices are obtained by super-imposition of two monochromatic lattices with slightly different wavelengths [7]. Manipulating the relative phase between the two standing waves and their respective depths independently, a periodic pattern of potential wells with two different depths at two adjacent sites is obtained. This difference in the depth of two adjacent sites is the measure of superlattice potential. In this report, we investigate spin-1 ultracold bosons loaded into 2-dimensional bi-chromatic optical superlattices.

MODEL AND METHOD

The spin-1 Bose-Hubbard model, which describes spin full bosons in an optical superlattice, is given by

$$\mathcal{H} = -t \sum_{\langle i,j \rangle, \sigma} (a_{i,\sigma}^\dagger a_{j,\sigma} + a_{j,\sigma}^\dagger a_{i,\sigma}) + \frac{U_0}{2} \sum_i \hat{n}_i (\hat{n}_i - 1) + \frac{U_2}{2} \sum_i (\vec{F}_i^2 - 2\hat{n}_i) - \sum_i \mu_i \hat{n}_i, \quad (1)$$

where first term represents hopping of bosons between nearest neighbour sites $\langle i, j \rangle$ with an amplitude t . Here $a_{i,\sigma}$ ($a_{i,\sigma}^\dagger$) represents annihilation (creation) operator at site i with spin projection $\sigma = \{-1, 0, 1\}$, number operator $\hat{n}_{i,\sigma} = a_{i,\sigma}^\dagger a_{i,\sigma}$ and $\hat{n}_i = \sum_\sigma \hat{n}_{i,\sigma}$. Spin operator $\vec{F}_i = (F_i^x, F_i^y, F_i^z)$ where $F_i^\alpha = \sum_{\sigma, \sigma'} a_{i,\sigma}^\dagger S_{\sigma, \sigma'}^\alpha a_{i,\sigma'}$ with $\alpha = x, y, z$ and $S_{\sigma, \sigma'}^\alpha$ are standard spin-1 matrices. Spin independent (dependent) interaction U_0 (U_2) arises due to the difference in the scattering length a_0 and a_2 in the spin S=0 and S=2 channels respectively. The spin dependent interaction U_2 can be positive (anti-ferromagnetic) or negative (ferromagnetic) depending on the values of a_0 and a_2 [5]. The site dependent chemical potential $\mu_i = \mu + (-1)^i \delta$ where μ controls the bosons density and δ is the shift in energy due to superlattice potential. Here, we consider a bi-chromatic superlattice and thus, the whole lattice is bipartite into A and B sub-lattices with $\mu_A = \mu + \delta$ and $\mu_B = \mu - \delta$.